

Course Work for 'Adaptive Full State Observer for Nonsalient PMSM with Noised Measurements of the Current and Voltage'

Yu Youyang

293834

I. INTRODUCTION

ORIGINAL paper introduces an adaptive algorithm for estimating magnetic flux in non-salient permanent magnet synchronous motors (PMSMs) with electrical signal offsets. Using a novel nonlinear parameterization via the dynamical regressor extension and mixing (DREM) procedure, the flux estimation problem is reformulated to identify constant parameters linked to measurement errors. The algorithm ensures the flux observation error converges to a bounded set with position error converging to zero, achieving global exponential convergence under persistent excitation and global asymptotic convergence otherwise. In this paper, noises in the measurable signals are investigated, and the anti-noise ability of this observer is studied by applying four different noises. From the experiments, this observer has good anti-interference ability to high frequency and low frequency noises. It has poor anti-jamming ability to Random noises with zero mean and Random noises with non-zero mean.

II. PROBLEM FORMULATION

Consider the classical, two-phase $\alpha\beta$ model of the unsaturated, non-salient PMSM in the stationary frame

$$\begin{aligned}\dot{\lambda}_{\alpha\beta} &= v_{\alpha\beta} - R i_{\alpha\beta}, \\ J_m \dot{\omega} &= -B\omega + \tau_e - \tau_L, \\ \dot{\theta} &= \omega,\end{aligned}\quad (1)$$

where $\lambda_{\alpha\beta} \in \mathbb{R}^2$ is the total flux,
 $i_{\alpha\beta} \in \mathbb{R}^2$ are the stator currents,
 $v_{\alpha\beta} \in \mathbb{R}^2$ are the stator voltages,
 $R > 0$ is the stator windings resistance,
 $J_m > 0$ is the rotor inertia,
 $\theta \in \mathbb{S} := [0, 2\pi)$ is the rotor phase,
 $\omega \in \mathbb{R}$ is the mechanical angular velocity,
 $B \geq 0$ is the viscous friction coefficient,
 $\tau_L \in \mathbb{R}$ is the—possibly time-varying—load torque,
 τ_e is the torque of electrical origin.
 The total flux of the surface-mounted PMSM verifies

$$\lambda_{\alpha\beta} = L i_{\alpha\beta} + \lambda_m \begin{bmatrix} \cos(n_p \theta) \\ \sin(n_p \theta) \end{bmatrix}, \quad (2)$$

where $L > 0$ is the stator inductance, λ_m is the constant flux generated by permanent magnets and $n_p \in \mathbb{N}$ is the number of pole pairs. Let's abbreviate $i_{\alpha\beta}$ to i for simplicity.

Assume the only signals available for measurements are the current i and the voltage v , which are corrupted by constant unknown bias terms $\delta_i \in \mathbb{R}^2$ and $\delta_v \in \mathbb{R}^2$, respectively, that is

$$\begin{cases} i_m = i + \delta_i \\ v_m = v + \delta_v \end{cases} \quad (3)$$

where i_m and v_m are actually measured signals. The resistance R and the inductance L are assumed to be known.

The goal is to reconstruct asymptotically the total flux λ with asymptotic convergence of estimation errors to 0. It is also very necessary to investigate noises in the measurable signals.

A. Model reparameterization

The adaptive flux observer for PMSM was based on the equation

$$|\lambda - L i|^2 - \lambda_m^2 = 0, \quad (4)$$

which follows from (2).

Expanding expressions (4) fields as

$$\lambda^\top \lambda - 2L \lambda^\top i_m + L^2 i_m^\top i_m + \lambda^\top \eta_1 + i_m^\top \eta_2 + \eta_3 = 0, \quad (5)$$

where $\eta_1 = 2L\delta_i$, $\eta_2 = -2L^2\delta_i$, $\eta_3 = L^2\delta_i^\top \delta_i - \lambda_m^2$ are constants that are unknown.

Differentiate (5) fields as

$$2\dot{\lambda}^\top \lambda - 2L(\dot{\lambda}^\top i_m + \lambda^\top \dot{i}) + 2L^2 \dot{i}_m^\top i_m + \dot{\lambda}^\top \eta_1 + \dot{i}_m^\top \eta_2 = 0, \quad (6)$$

Then apply the filter $\frac{\nu}{p+\nu}$, where $p := \frac{d}{dt}$ is a differential operator. And then using the Swapping Lemma to get the regressor equation where the flux λ and vector η enter linearly only. Finally apply the filter $\frac{p}{p+\nu}$. Rewriting obtained operator expression as ordinary differential equations to get following equations

$$\begin{aligned}\dot{\xi}_1 &= -\nu \xi_1 + 2\nu y_m + 2\nu^2 L i_m, \\ \dot{\xi}_2 &= -\nu \xi_2 + \xi_1 + 2y_m, \\ \dot{\xi}_3 &= -\nu \xi_3 + y_m^\top \xi_1 + \nu^2 L^2 i_m^\top i_m, \\ \dot{\xi}_4 &= -\nu \xi_4 + \nu \xi_2 - \xi_1, \\ \dot{\xi}_5 &= -\nu \xi_5 + \nu \xi_3 - \nu^2 L^2 i_m^\top i_m + y_m^\top (\nu \xi_2 - \xi_1),\end{aligned} \quad (7)$$

Select $y_m = -Ri_m + v_m$, and define

$$\begin{aligned} y &= \xi_3 - \nu L^2 i_m^\top i_m - \xi_5, \\ \Phi &= 2\xi_1 - 2\nu L i_m - \nu \xi_2, \\ \Psi &= \begin{pmatrix} 2\xi_4 \\ 2\nu^{-1} \end{pmatrix}. \end{aligned} \quad (8)$$

According to Proposition 1, the following regression model holds

$$\begin{aligned} \dot{\lambda} &= -Ri_m + v_m + \eta_m, \\ y &= \Phi^\top (\lambda + \frac{1}{2}\eta_1) + \Psi^\top \eta + \varepsilon_t, \end{aligned} \quad (9)$$

where the known functions y, Φ, Ψ are computed from available signals, $\eta_m := R\delta_i - \delta_v$ and $\eta_m := (\eta_{m1} \ \eta_{m2} \ \eta_m^\top \eta_m)^\top$ are unknown constant vectors and ε_t is an exponentially decaying term.

B. DREM-based estimator

Now, it is necessary to estimate the unknowns. Directly, the DREM procedure is not applicable to the model (9) since λ is a function of time.

Step 1. Extension

In accordance with DREM we need to form $\dim(\lambda + \frac{1}{2}\eta_1) + \dim(\eta) - 1 = 4$ new regression models with different filter $\frac{\alpha}{p+\alpha}$ with the coefficient $\alpha > 0$ from the original one (9)

$$\begin{aligned} \frac{\alpha}{p+\alpha}y &= \frac{\alpha}{p+\alpha}\Phi^\top (\lambda + \frac{1}{2}\eta_1) + \frac{\alpha}{p+\alpha}\Psi^\top \eta \\ &= (\lambda + \frac{1}{2}\eta_1)^\top \frac{\alpha}{p+\alpha}\Phi - \frac{1}{p+\alpha} \left(\dot{\lambda}^\top \frac{\alpha}{p+\alpha}\Phi \right) + \eta^\top \frac{\alpha}{p+\alpha}\Psi \\ &= (\lambda + \frac{1}{2}\eta_1)^\top \frac{\alpha}{p+\alpha}\Phi - \frac{1}{p+\alpha} \left((v_m - Ri_m + \eta_m)^\top \frac{\alpha}{p+\alpha}\Phi \right) \\ &\quad + \eta^\top \frac{\alpha}{p+\alpha}\Psi = (\lambda + \frac{1}{2}\eta_1)^\top \frac{\alpha}{p+\alpha}\Phi - \frac{1}{p+\alpha} \left(y_m^\top \frac{\alpha}{p+\alpha}\Phi \right) \\ &\quad - \eta_m^\top \frac{\alpha}{(p+\alpha)^2}\Phi + \eta_m^\top \frac{\alpha}{p+\alpha}(2\xi_4) + \eta_m^\top \eta_m \frac{\alpha}{p+\alpha}(2\nu^{-1}) \end{aligned} \quad (10)$$

Rewrite as

$$z_\alpha = \bar{\Phi}_\alpha^\top (\lambda + \frac{1}{2}\eta_1) + \bar{\Psi}_\alpha^\top \eta \quad (11)$$

where

$$\begin{aligned} z_\alpha &= \frac{\alpha}{p+\alpha}y + \frac{1}{p+\alpha} \left(y_m^\top \frac{\alpha}{p+\alpha}\Phi \right), \\ \bar{\Phi} &= \frac{\alpha}{p+\alpha}\Phi, \\ \bar{\Psi} &= \left(\frac{\alpha}{p+\alpha}(2\xi_4) - \frac{\alpha}{(p+\alpha)^2}\Phi \right). \end{aligned} \quad (12)$$

Step 2. Mixing

According to Step 1.Extension, we can mix the new regression model and obtain the extended regression,

$$Z(t) = M(t) \begin{pmatrix} \lambda(t) + \frac{1}{2}\eta_1 \\ \eta \end{pmatrix}, \quad (13)$$

where

$$Z(t) := \begin{pmatrix} y(t) \\ z_1(t) \\ \vdots \\ z_N(t) \end{pmatrix}, \quad M(t) := \begin{pmatrix} \Phi^\top & \Psi^\top \\ \bar{\Phi}_1^\top & \bar{\Psi}_1^\top \\ \vdots & \vdots \\ \bar{\Phi}_N^\top & \bar{\Psi}_N^\top \end{pmatrix}.$$

The next step is to obtain a set of scalar N equations as follows,

$$\begin{aligned} \text{adj}M(t)Z(t) &= \text{adj}M(t)M(t) \begin{pmatrix} \lambda(t) + \frac{1}{2}\eta_1 \\ \eta \end{pmatrix} \\ &= \det M(t) \begin{pmatrix} \lambda(t) + \frac{1}{2}\eta_1 \\ \eta \end{pmatrix} \end{aligned}$$

Then split it to 2 rows as

$$Y_\lambda(t) = \Delta(t)(\lambda(t) + \frac{1}{2}\eta_1), \quad (14)$$

$$Y_\eta(t) = \Delta(t)\eta,$$

where

$$Y(t) := \begin{pmatrix} Y_\lambda(t) \\ Y_\eta(t) \end{pmatrix} = \text{adj}M(t) Z(t),$$

$$\Delta(t) := \det M(t).$$

To estimate η we use the classical gradient algorithm as Proposition 2,

$$\dot{\hat{\eta}} = \gamma_\eta \Delta (Y_\eta - \Delta \hat{\eta}), \quad (15)$$

As seen from (14) the estimate of flux is affected by the unknown parameter η_1 which is proportional to the unknown constant bias of currents δ_i . Therefore, the paper considers the following three scenarios to construct the flux observer:

- 1) δ_i is known and δ_v is unknown;
- 2) δ_i is unknown and δ_v is known;
- 3) both δ_i and δ_v are unknown.

For first scenarios, original paper construts following model,

$$\begin{aligned} \hat{\lambda} &= \chi - L\delta_i, \\ \dot{\chi} &= -Ri_m + v_m + \hat{\eta}_m + \gamma_\lambda \Delta (Y_\lambda - \Delta \chi) \end{aligned} \quad (16)$$

For seconed scenarios, original paper construts following model,

$$\begin{aligned} \hat{\lambda} &= \chi - \frac{L}{R}(\hat{\eta}_m + \delta_v), \\ \dot{\chi} &= -Ri_m + v_m + \hat{\eta}_m + \gamma_\lambda \Delta (Y_\lambda - \Delta \chi) \end{aligned} \quad (17)$$

For third scenarios, original paper construts following model,

$$\begin{aligned} \hat{\lambda} &= \chi - \frac{L}{R}\hat{\eta}_m, \\ \dot{\chi} &= -Ri_m + v_m + \hat{\eta}_m + \gamma_\lambda \Delta (Y_\lambda - \Delta \chi), \end{aligned} \quad (18)$$

C. Position and speed observer

The unknown position is reconstructed by the following. Replacing (3) in (2) we obtain

$$\lambda = Li_m - L\delta_i + \lambda_m C(\theta). \quad (19)$$

Because $\eta_1 = 2L\delta_i$ and as seen from (16), (17) and (18) the estimate of the signal $(\lambda + \frac{1}{2}\eta_1)$ is generated by the signal χ . We obtain following equation

$$\hat{\theta}(t) = \frac{1}{n_p} \arctan \left(\frac{\chi_2 - Li_{m2}}{\chi_1 - Li_{m1}} \right). \quad (20)$$

The rotor speed can be estimated from the observed position $\hat{\theta}$ with the help of a standard phase-locked loop (PLL) speed estimator

$$\begin{aligned} \dot{\chi}_1 &= K_p(\hat{\theta} - \chi_1) + K_i\chi_2, & \dot{\chi}_2 &= \hat{\theta} - \chi_1, \\ \hat{\omega} &= K_p(\hat{\theta} - \chi_1) + K_i\chi_2, \end{aligned}$$

where $K_p > 0$ and $K_i > 0$ are proportional and integral gains, respectively.

This PLL-type speed estimator is constructed from angle error $\hat{\theta} - \chi_1$. The estimator uses PLL angle χ_1 and PLL angle error χ_2 . Using these two new variables we form a tracking controller consisting of a PI regulator and an integrator. The PI gains of the controller are K_p and K_i . Motivation of the PI regulator application stems from the fact that PI controllers have the ability of suppressing error under the presence of a disturbance.

III. IMPLEMENTATION IN MATLAB

Firstly the PMSM model with constant unknown bias term and vector control in constructed in Simulink in Figure 1.

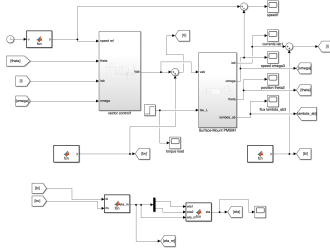


Fig. 1: the PMSM model with constant unknown bias term and vector control

And then construct the regression model (9) in Figure 2.

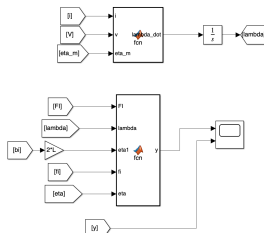


Fig. 2: regression model (9)

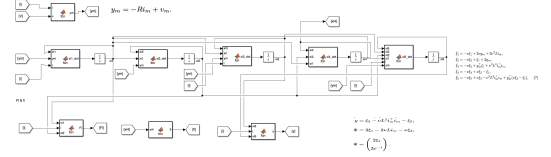


Fig. 3: differential equations(7)

And to find the $\bar{\Phi}$ and $\bar{\Psi}$ construct the differential equations (7) in Figure 3.

Then using DREM method, to construct the Step 1 extension in Figure 4.

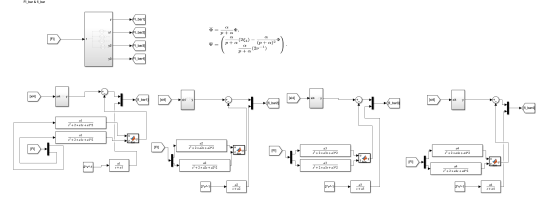


Fig. 4: DREM: Step 1 extension

Then to Construct the Step 2 mixing in Figure 5.

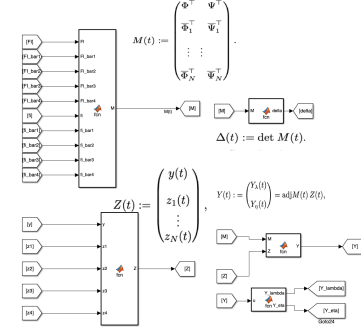


Fig. 5: DREM: Step 2 mixing

To estimate η , construct the SGD model(15) for it in Figure 6.

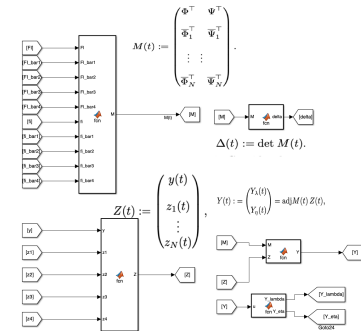


Fig. 6: SGD model

According to (16) (17) (18) to build flux observer for three scenarios in Figure 7.

Finally to estimate the position and the speed, we build the position observer and PLL observer for speed in Figure 8.

So far, the reproduction work in Matlab is finished.

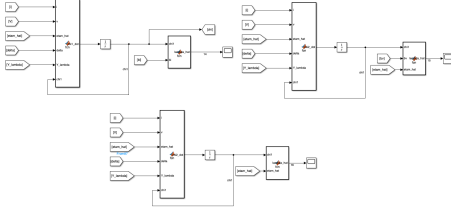


Fig. 7: flux observer for 3 scenarios



Fig. 8: position and speed estimator

IV. RESULTS

In this section, the parameters of PMSM motor are listed in Table 1. The motor is controlled by classical field-oriented controller. The desired motor speed increases linearly from 0 rad/sec to 523 rad/sec during the time interval $t \in (0; 0.2)$ sec and then remains constant. The external load torque applied to the motor is zero at the start and $\tau_L = 1N \cdot m$ after 0.3 sec.

TABLE I: Parameters of the first motor BMP0701F

| Parameter (units) | Motor |
|-------------------------------------|---------------------|
| Inductance L (mH) | 40.03 |
| Drive inertia j (kgm ²) | 60×10^{-6} |
| Pairs of poles np (-) | 5 |
| Magnetic flux λ_m (Wb) | 0.2086 |

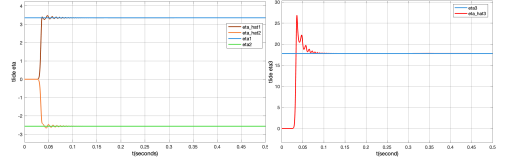
And initial parameters and design parameters in the procedure (15) (16) (17) (18) are listed in Table 2.

TABLE II: Parameters of other parameters

| Parameter (units) | Motor |
|-------------------------------|-------------|
| $\lambda^T(0)$ | [0.2086 0] |
| $\omega(0), \theta(0), i(0)$ | 0 |
| $\hat{\eta}^T(0)$ | [0 0 0] |
| $\chi^T(0)$ | [0 0] |
| v | 1400 |
| α_1 | 80 |
| α_2 | 200 |
| α_3 | 360 |
| α_4 | 520 |
| $\gamma_\eta, \gamma_\lambda$ | 1 |
| K_p | 2000 |
| K_i | 10000 |
| δ_v^T | [0.4 - 0.3] |
| δ_v | [0.2 - 0.1] |

In Figure 9 the transient processes for the estimates $\hat{\eta}^T = [\hat{\eta}_1 \ \hat{\eta}_2 \ \hat{\eta}_3] = [\hat{\eta}_{m1} \ \hat{\eta}_{m2} \ \hat{\eta}_m^T \ \hat{\eta}_m]$ are shown. As seen, the parameter estimates converge to their true values fast. The estimates $\hat{\eta}_1$ and $\hat{\eta}_2$ perform very low oscillations. The estimate $\hat{\eta}_3$ exhibits an overshoot at the beginning, then shows small fluctuations and goes to the true value.

Figure 10 illustrates the transients of the absolute value of the flux observation error for the algorithms (14), (15) and (16), respectively. As seen from simulation results, observers (14) and (15) perform fast convergence of the flux error to zero.

Fig. 9: estimation of parameters $\hat{\eta}_1, \hat{\eta}_2$ and $\hat{\eta}_3$

The transient behavior of the observer (16) is similar to the observers (14) and (15). And there is a low stationary error in the steady state which coincides with analytically calculated bound.

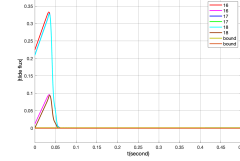


Fig. 10: absolute value of the flux observation error

Figure 11 demonstrates the transients of the estimation error for position estimator and PLL estimator for speed.

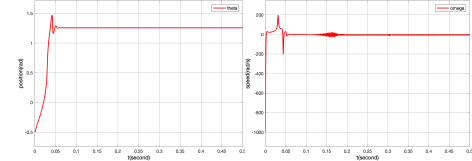
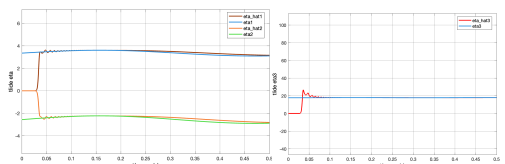


Fig. 11: error for position estimator and PLL estimator for speed

Now to investigate noises in the measurable signals. There are four kinds of noise as following: 1) Low frequency noises 2) High frequency noises 3) Random noises with zero mean 4) Random noises with non-zero mean

For the first kind of noise: low frequency noises, I set $\epsilon_v^T = [0.01\sin(0.1t) \ 0.02\sin(0.1t)]$ and $\epsilon_i^T = [0.03\sin(0.1t) \ 0.04\sin(0.1t)]$, where ϵ is noises in the measurable signals. Figure 12 shows the transient processes for the estimates $\hat{\eta}^T = [\hat{\eta}_1 \ \hat{\eta}_2 \ \hat{\eta}_3] = [\hat{\eta}_{m1} \ \hat{\eta}_{m2} \ \hat{\eta}_m^T \ \hat{\eta}_m]$ under the low frequency noises. And Figure 13 shows the flux observation error under the low frequency noises. Similarly, as in the absence of noise, the parameter converges quickly. With the superposition of noise, the measured value will continue to increase, and the estimated value will deviate, so the measured value cannot be tracked. However, it has a good ability to resist low-frequency noise in a certain period of time. But this error model does not converge to 0 as time tends to infinity.

Fig. 12: $\hat{\eta}^T$ under the low frequency noises.

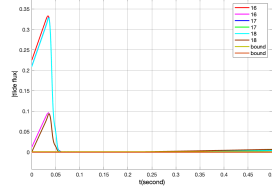


Fig. 13: $|\tilde{\lambda}(t)|$ under low frequency noises

For the second kind of noise: high frequency noises, I set $\epsilon_v^\top = [0.01\sin(t) \ 0.02\sin(0.001t)]$ and $\epsilon_i^\top = [0.03\sin(t) \ 0.04\sin(0.001t)]$. Figure 14 shows the transient processes for the estimates $\hat{\eta}^\top = [\hat{\eta}_1 \ \hat{\eta}_2 \ \hat{\eta}_3] = [\hat{\eta}_{m1} \ \hat{\eta}_{m2} \ \hat{\eta}_m^\top \hat{\eta}_m]$ under the high frequency noises. When noise is added, the measured value of $\hat{\eta}^\top$ fluctuates, and the estimated value also fluctuates, but it can be clearly seen that the fluctuation of the predicted value is much smaller than that of the measured value, indicating that the model maintains good robustness under the disturbance of high-frequency noise. Figure 15 shows the flux observation error under the high frequency noises. When noise is added, the flux observation error still converges to 0 at 0.25s despite high frequency vibration.

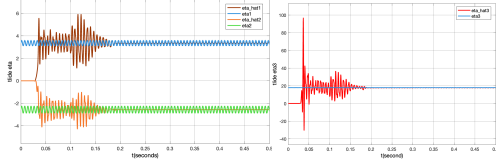


Fig. 14: $\hat{\eta}^\top$ under the high frequency noises.

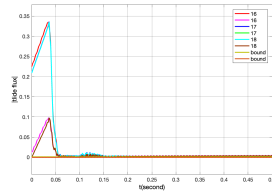


Fig. 15: $|\tilde{\lambda}(t)|$ under high frequency noises

For the third kind of noise: random noises with zero mean, I used Band-Limited White Noise block to set ϵ^\top with noise power of 0.001 and a sampling time of 0.01. Figure 16 shows the transient processes for the estimates $\hat{\eta}^\top = [\hat{\eta}_1 \ \hat{\eta}_2 \ \hat{\eta}_3] = [\hat{\eta}_{m1} \ \hat{\eta}_{m2} \ \hat{\eta}_m^\top \hat{\eta}_m]$ under the white noises. After the white noise is applied, the fluctuation of $\hat{\eta}^\top$ is very large, and the estimated value can track the measured value quickly, but the estimated value has a very large oscillation at the beginning. This shows that the anti-noise ability is very poor within 0-0.2s, but the anti-noise ability is good after 0.2s. Compared with the previous two kinds of noise, the error is large. Figure 17 shows the flux observation error under the white noises. It clearly shows that the addition of white noise prevents $|\tilde{\lambda}(t)|$ from converging to 0 normally and from being consistent with bound.

For the fourth kind of noise: random noises with none-zero mean, I used pink block to set ϵ^\top with seed of 67, mean of 0.05

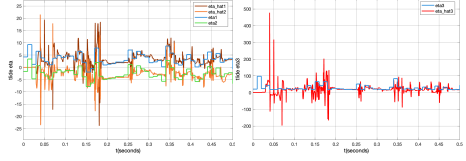


Fig. 16: $\hat{\eta}^\top$ under the white noises.

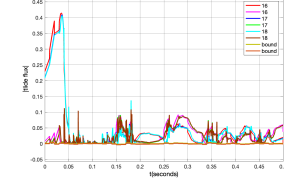


Fig. 17: $|\tilde{\lambda}(t)|$ under white noises

and a sampling time of 0.01. Figure 18 shows the transient processes for the estimates $\hat{\eta}^\top = [\hat{\eta}_1 \ \hat{\eta}_2 \ \hat{\eta}_3] = [\hat{\eta}_{m1} \ \hat{\eta}_{m2} \ \hat{\eta}_m^\top \hat{\eta}_m]$ under the pink noises with none-zero mean. After adding the random noise with non-zero mean, the change of $\hat{\eta}^\top$ is similar to that of the zero mean noise, with a large oscillation at the beginning, and then it can track the measurement. Figure 19 shows the similar condition of flux observation error under the white noises. In a word, the model performs poorly against random noise.

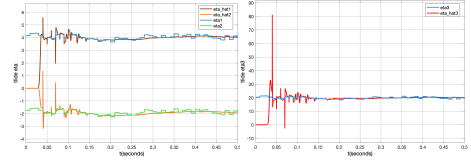


Fig. 18: $\hat{\eta}^\top$ under the pink noises with 0.05 mean value.

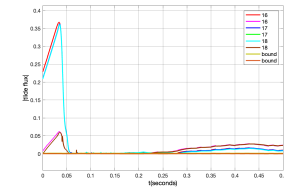


Fig. 19: $|\tilde{\lambda}(t)|$ under pink noises with 0.05 mean value

V. CONCLUSIONS

In the original paper, they proposed a new adaptive observer design algorithm that allows parametrizing the perturbed PMSM model into a linear regression equation with respect to the observed flux, with terms related to the current bias and constant offsets related to the measurement error, bias or offset. Using the DREM method, a vector regression equation can be decomposed into a set of scalar regression equations with common measurable regressors and unknown variables or parameters. In this paper, I reproduce their result and prove the superiority of this adaptive observer. At the same time, I carried out an investigation on noises in the measurable signals. By simulating four different types of noise signals

in Matlab and applying them to the deviation of voltage and current, I checked the anti-noise ability of the model. The experimental results show that the model has good ability to resist high frequency noise signal and low frequency noise signal, but has poor ability to resist random signal with or not with zero mean.